Jurnal Teknologi

Full Paper

MECHANOSYNTHESIS, CRYSTAL STRUCTURE, MAGNETIC AND ABSORPTION PROPERTIES OF Al SUBSTITUTED $BaFe_{12}O_{19}$

Didin S. Winatapura*, Deswita, Adel Fisli, Wisnu Ari Adi

Center for Science and Technology of Advanced Materials, National Nuclear Energy Agency (BATAN), Kawasan Puspiptek, Serpong, Tangerang 15314 - Indonesia

Article history
Received
28 January 2019
Received in revised form
29 May 2019
Accepted
17 June 2019
Published online
26 August 2019

*Corresponding author
didinsw@batan.go.id

Graphical abstract

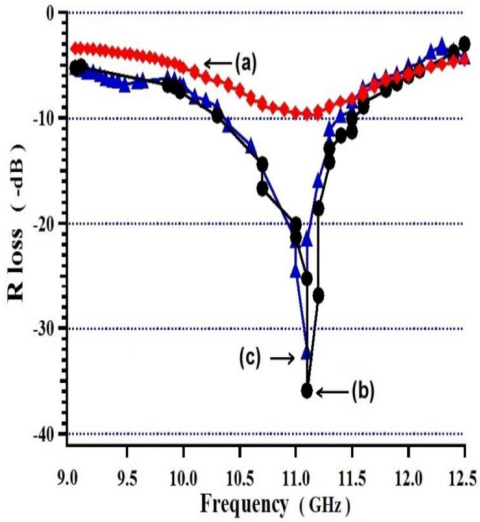

Abstract

The Aluminums (Al) substituted on M-type barium ferrite ($BaFe_{12}O_{19}$) is one of the magnetic materials, which can be applied to the microwave band working at high frequencies. The purpose of this paper is to investigate the effect of Al substitution for Fe^{3+} ions on the structure, magnetic and absorption behavior of M-type barium ferrite. The sample was prepared by mechano-synthesis using high-energy milling (HEM). In this research, Fe ion in $BaFe_{12}O_{19}$ was substituted by Al ion to form $BaFe_{12-x}Al_xO_{19}$ for x = 0.0, $BaFe_{10}Al_2O_{19}$ for x = 2.0 and $BaFe_8Al_4O_{19}$ for x = 4.0 which is called as BAl-0, BAl-2 and BAl-4 sample, respectively. The stainless steel balls were used for the milling with a ball-to-powder sample ratio of 5. The mixing and milling for each the sample was conducted for 5 hours in ethanol medium and dried at 100°C in oven for 24 hours and then followed by heat treatment at 1100°C during 1h in the atmosphere media. The sample was characterized using X-rays diffractometer (XRD), Scanning Electron Microscope (SEM), Vibrating Sample Magnetometer (VSM) and Vector Network Analyzer (VNA). The result indicates that the addition of Al ion lead to the change cell parameters, volume, and the particles size. The magnetic behavior such as magnetic coercivity (H_c), magnetization saturation (M_s) and remanent (M_r) changed significantly with the substitution of Al ions. The optimum reflection loss (RL) is found to be –35dB at 14GHz for $BaFe_{10}Al_2O_{19}$ (BAl-2) sample. It is shown that Al substitutions change the particle size, ferromagnetic resonant frequency, and structural and magnetic behavior of M-type barium ferrite.

Keywords: $BaFe_{12}O_{19}$, mechano-synthesis, reflection loss, absorption, crystal structure, magnetic properties

© 2019 Penerbit UTM Press. All rights reserved

1.0 INTRODUCTION

M-type ferrite, $BaFe_{12}O_{19}$ has been widely investigated owing to its interesting properties such as excellent chemical stability, corrosion resistance and high magnetic properties (high saturation magnetization, high coercivity, high magneto-crystalline anisotropy). The M-type $BaFe_{12}O_{19}$ hexagonal ferrite in substituted form is well suited to applications in the microwave absorbing materials because it can be used at much higher frequency range (GHz) than the ferrites with spinel and garnet structure [1–3]. However, the resistivity of $BaFe_{12}O_{19}$ is very high, so the main absorbing mechanism is magnetic loss. The magnetic loss of $BaFe_{12}O_{19}$ derives from their magnetic properties, the resonance

absorption of moving magnetic domains, and spin relaxation at the high-frequency alternating electromagnetic fields.

It has been studied that an improvement in the intrinsic magnetic properties of $BaFe_{12}O_{19}$ can enhance their microwave absorbing ability [4–7]. In order to adjust the electromagnetic parameters and ferromagnetic resonant frequency of the pure $BaFe_{12}O_{19}$, various ions doping have been investigated intensively. Numerous papers have been reported on the study of structural, magnetic and microwave absorption properties. They explained that the structural, magnetic and absorption properties of $BaFe_{12}O_{19}$ can be improved by substituting Fe with ions such as Zn, Ti, Mn, Cr, La and Al [2, 3, 7–11].

In this paper, we report the structural changes (cell volume, lattice parameters and crystallite size) that may occur due to substitution of Al and also the effect on the magnetic (saturation magnetization, coercivity and remanence) properties of the materials synthesized by the mechanosynthesis method. The aim for the substitutions of Al is to synthesis the $BaFe_{(12-x)}Al_xO_{19}$ (x = 0.0, 2.0, and 4.0), and to study the influence of Al ion substitution on the structural, magnetic and microwave absorbing performance. The sample was characterized using an X-ray diffractometer (XRD), scanning electron microscopy (SEM) coupled with energy dispersive spectrophotometer (EDS), vibrating sample magnetometer (VSM), and vector network analyzer (VNA). In the present work, the our attention was focused on structural, magnetic and absorption properties of $BaFe_{(12-x)}Al_xO_{19}$ (x = 0.0, 2.0, and 4.0) as part of M-type barium ferrite.

2.0 METHODOLOGY

$BaFe_{12}O_{19}$ (BAl-0), $BaFe_{10}Al_2O_{19}$ (BAl-2), and $BaFe_8Al_4O_{19}$(BAl-4) samples were prepared using the high energy ball milling (Certi-prep 8000 mixer/mill). The staring raw materials used were analytical grade (manufactured by Sigma Aldrich) Fe_2O_3, $BaCO_3$ and Al_2O_3 powders of high purity (≥ 99.0%) The raw materials were weighted accurately (to four decimal places) in stoichiometric composition, and wet mixed in a stainless steel vials for 5 hours. The milling of the mixture was conducted under ethanol condition. The Stainless steel vials (45 ml volume and 50 mm inner diameter) were loaded with 10 g of powder and 12 stainless steel balls of 5 mm diameter each, resulting in a ball-to-powder mass ratio of 5:1. The milling of the mixture was conducted under ethanol condition. The precursor powders were dried at 100°C in oven for 24 hours and then shaped into pellet (diameter = 17.5 mm and thickness = 3 mm) using automatic axial hydraulic press at 1500 kgf/cm^2 pressure. For further crystal growth, the pellet was annealed in air atmosphere at temperatures 1100°C using a heating/cooling rate of 10°C min^{-1}. The precursor powders were dried at 100°C in oven for 24 hours, grounded with mortar agate and then shaped into a pellet (diameter = 17.5 mm and thickness = 3 mm) using automatic axial hydraulic press at 1500 kgf/cm^2 pressure. In the final stage, the pellet was sintered in air atmosphere at temperatures 1100°C using a heating/cooling rate of 10°C min^{-1}.

Phase distribution and unit cell variation were determined by means of powder X-ray diffraction (XRD) analysis in Phillips Panalytical PW1710 equipment together with the help of Fullprof program by employing Rietveld refinement technique. The particle size was calculated using Scherer formula. Scanning Electron Microscopy (SEM) observations in a JEOL JSM 6510 at 20 kV afforded verification of grain morphology and their mean size. The magnetic properties of all composition were collected in a room temperature by Vibrating Sample Magnetometer (VSM) in OXFORD 1.2T equipment at a maximum applied field of 1200 KA/m. The reflection loss of the absorber was measured as a function of frequency, using Vector Network Analyser (VNA) in ADVANTEST R3770 equipment in the frequency range of 9 – 13 GHz.

3.0 RESULTS AND DISCUSSION

X-ray powder diffraction patterns for all prepared samples are shown in Figure 1. All the peaks are indexed to M-type barium ferrite $BaFe_{12}O_{19}$. There is no any signature of secondary phases giving the impression that the samples are pure phase. The XRD patterns of all the samples were identified using JCPDS file number 00-043-0002. Based on the Figure 1, it can be seen that the XRD pattern of Figure 1(a) – 1(c) are very similar. They are composed of only M-type hexagonal barium ferrite. This condition revealed that during heat treatment, the Al ions enter to the lattice of barium ferrite. The crystallite sizes (D) of the samples calculated by Scherrer formula are found to be in the range from 60 to 80 nm. The XRD data is then analyzed using the Fullprof program by employing Rietveld refinement technique, as shown in Figure 2

The XRD patterns refinement of the sample was performed using the space group P63/mmc for hexagonal structure. The initial refinement was performed considering systemic errors in to account as zero-point shift, then unit cell and background parameters were refined. To further improve the fitting, all parameters such as the peak profile, thermal, lattice, scale factors, occupancy and atomic functional positions were refined. The background was corrected using a 12-Coefficientd Fourier cosine – series mode and the diffraction peak profiles were fitted by pseudo-Voigt function. A good agreement was obtained between experimental and calculated data. The structure parameters of the sample are presented in Table 1.

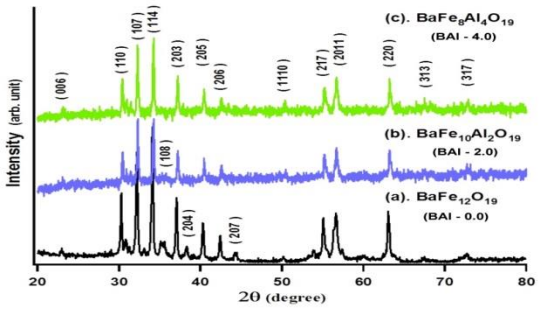

Figure 1 XRD patterns of (a). BAl-0, (b). BAl-2, and (c). BAl-4 sample

The quality fitting with χ^2 (chi-squared) is allowed a maximum of 1.3. With Al^{3+} substitutions, the value of '*a*' slightly but the value of '*c*' increase and decreases due to difference in ionic radii of Fe^{3+} ion (0.645Å) dan Al^{3+} ion (535Å).

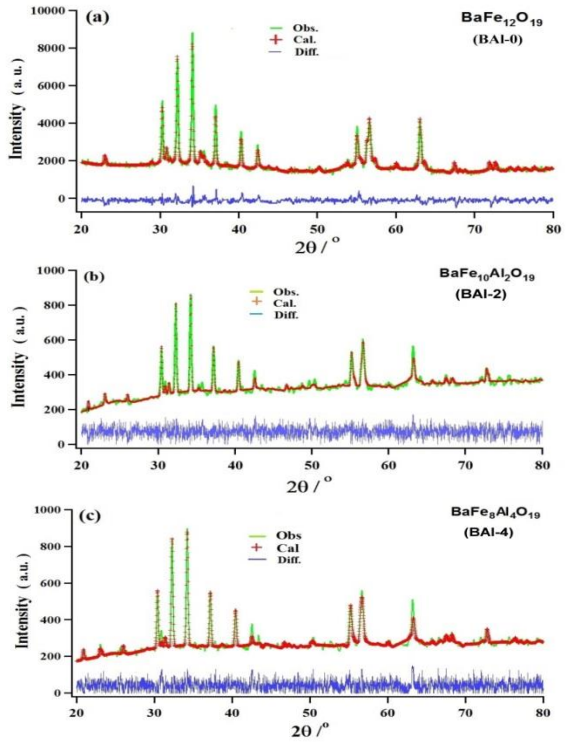

Figure 2 XRD refinement patterns of M-type barium ferrite in (a). BAl-0, (b). BAl-2, and (c). BAl-4 sample. X-ray calculations data are shown as plus red marks, the green solid lines are the observations data, and the blue solid lines (lowest curve) represent the difference between the observed and calculated profiles

Figure 2(a)-(c) show the result of the Rietveld refinement of $BaFe_{(12-x)}Al_xO_{19}$ powder for BAl-0 (x=0), BAl-2 (x=2), and BAl-4 (x=4.0). The peak intensities are in accordance with literature data [12]. The refined structural parameters such as lattice constants (*a*, *c*), the density (ρ) and unit cell volume (V_{cell}) obtained from Rietveld refinement for all the samples are shown in Tables 1. It is observed that the lattice constants "a", the density (ρ) and cell volume (*Vcell*) decease with an increase of Al content (x), while lattice constants "c" is slightly increase and then decease with Al content (x). This is mainly due to the fact that the ionic radii of Al^{3+} ions (0.535 Å) are smaller than that of Fe^{3+} ions (0.645 Å) which causes lattice shrinkage and reduces crystallite size. The change of the structure parameter is in agreement with that reported by Mahadevan *et al*. [9], Yang *et al*. [11] and Trukhanov *et al*. [14].

Table 1 The structure parameter of sample

Sample	*a* (Å)	*c* (Å)	V_{cell} (Å^3)	ρ(g.cm^{-3})
BAl-0	5.887	23.132	694.330	11.034
BAl-2	5.879	23.151	692.955	11.015
BAl-4	5.872	23.121	690.409	10.547

The crystallite size "D" could be calculated using Debye scherrer equation:

$$D = \frac{0.9\lambda}{\beta \cos\theta} \quad \ldots\ldots\ldots\ldots\ldots\ldots\ldots\ldots\ldots\ldots \quad (1)$$

Where β = FWHM (full-width at half maximum of the peak), λ = 1.5406 Å (Cu-Kα), θ is the Bragg's angle. The FWHM was obtained from observation FWHM minus FWHM standard of equipment. The result of crystallite size, D was mentioned in in Figure 3. The crystallite size, D of the sample was obtained of 69nm (BAl-0), 73 nm (BAl-2) and 67 (for BAl-4). It is shown that the average crystallite size D not change significantly, slightly increase and then decrease with Al content (x).

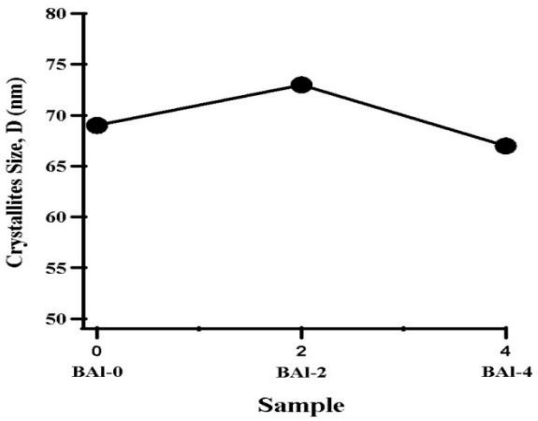

Figure 3 Average crystallites size, D of the samples

Figure 4 shows the SEM microstructure of the surface from different Al substitution in BAl-0, BAl-2 and BAl-4 sample. The images present a heterogeneous distribution of grain sizes. The grains appear to stick to each other. Some grains agglomerate in different masses. The surface of all sample appear to be dense, but it contains irregularly shaped particles.

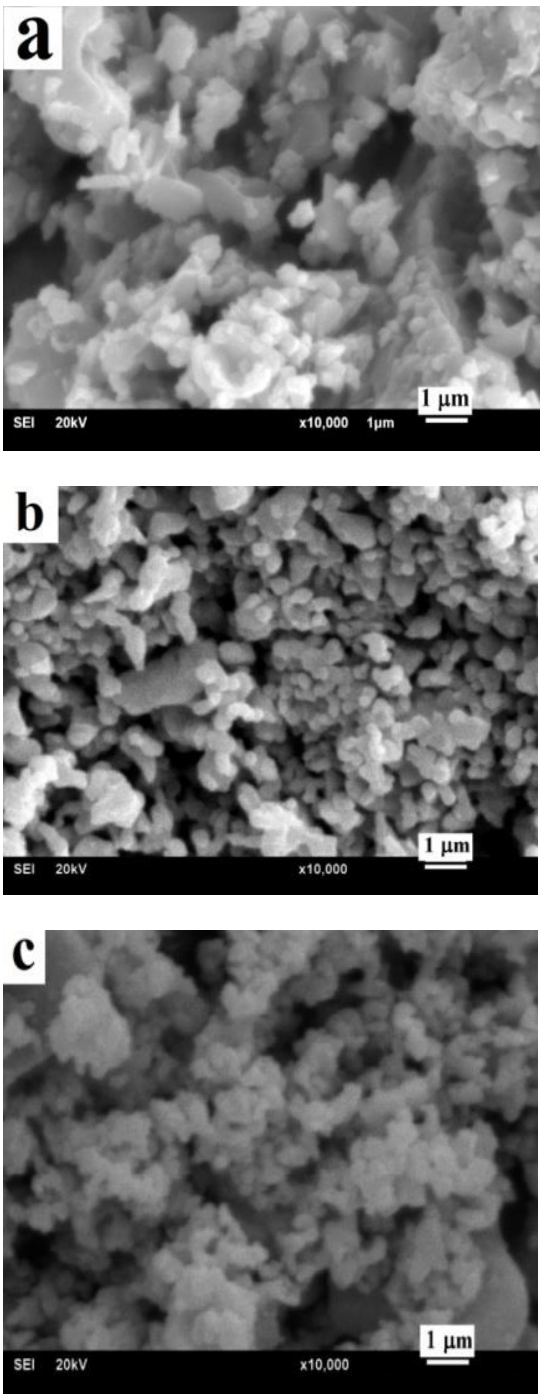

Figure 4 SEM images of M-type barium ferrite of (a). BAl-0, (b). BAl-2, and (c). BAL-4

Figure 5 display the room temperature M–H hysteresis loops of BAl-0, BAl-2 and BAl-4 samples, respectively. The saturation magnetization (M_s), remanent magnetization (M_r) and coercivity (H_c) of the magnetic powders samples are determined from the obtained hysteresis loops and their values are summarized in Table 2. It is seen that the changes of the saturation (M_s) and remanent magnetization (M_r) as a function of Al content (x). It is found that both M_s and M_r of the magnetic powders basically decrease with increasing Al content (x) from 0 to 4.0. The change of M_s and M_r with Al content (x) is in agreement with that reported by Mahadevan *et al*. [9] and Yujie Yang *et al*. [11]. The magnetization of $BaFe_{12}O_{19}$ (BAl-0) was reached of 88emu.g^{-1} which comes from the contribution of Fe^{3+} ions in the sample. This is greater than the theoretically magnetization value of 72emu.g^{-1}. Additionally, substitution my cause the M_s Value steep declined to 45emu.g^{-1} and 43emu.g^{-1} for BAl-2 (x=2.0) and BAl-4 (x=4.0) samples, respectively. The condition indicates that Fe^{3+} ions are replaced by Al^{3+} ions when Al combines into M-type ferrite. This could be understood that Fe^{3+} ions carrying a magnetic moment (~5μ_B) are replaced by Al^{+3} having magnetic moment, 0μ_B. The decrease in M_s is due to the present of large amount anti-ferromagnetic Al^{+3} ions. This non-magnetic Al^{+3} ions would decrease the Fe^{3+}-O-Fe^{3+}super exchange interaction to result in a decrease in the net magnetic moment per unit cell.

The variation of the coercivity (H_c) as a function of Al content (x) for BAl-0, BAl-2 and BAl-4 samples magnetic powders are shown in Table 2. The H_c value of 4.20 kOe was observed in the $BaFe_{12}O_{19}$ (BAl-0) sample for Al content (x) = 0.0, which is due to uniaxial magnetocrystalline anisotropy along c-axis. It is observed that there is a significant fall in H_c from 4.20kOe at Al content (x) = 0 to H_c = 3.13 kOe and H_c = 2.85kOe for BAl-2 and BAl-4 samples, respectively. The coercivity decreased with the increase in Al^{3+} content due to decrease in magneto-crystalline anisotropy [3, 8, 10, 13]. Our results on the magnetic properties of Al^{3+} substituted $BaFe_{(12-x)}Al_xO_{19}$ M-type ferrite for x = 2.0, and x = 4.0 are in good agreement with those already reported for the substituted barium hexaferrite (Al, Cr) [15]. Consequently, a decrease in H_c with an increase in Al^{3+} content is expected behavior for a magnetic microwave absorber application.

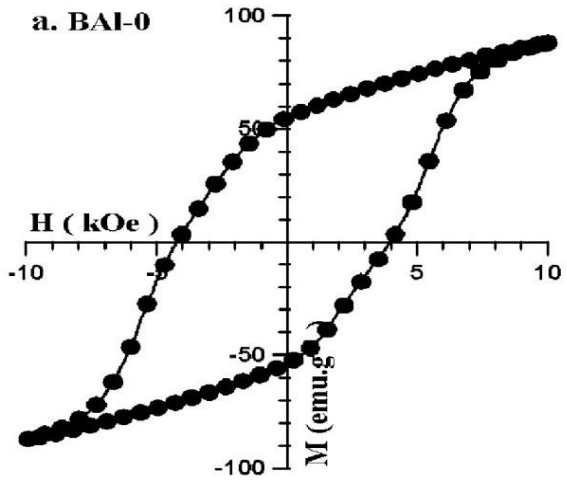

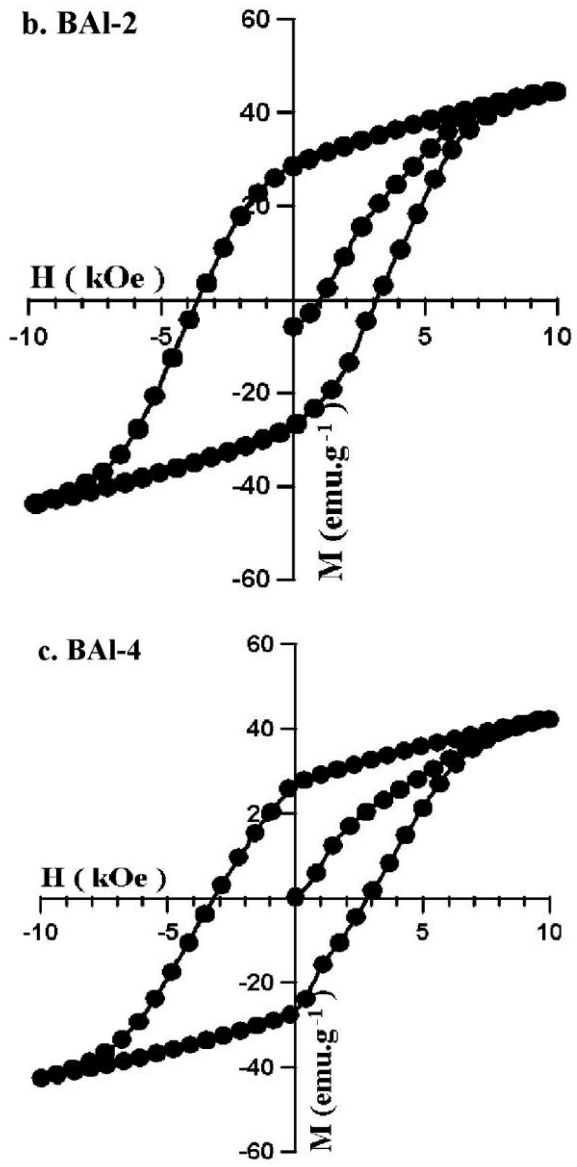

Figure 5 The hysteresis loop of M-type barium ferrite of (a). BAl-0, (b). BAl-2, and (c). BAl-4 samples

Table 2 The magnetic properties of sample

Sample	H_c (kOe)	M_s (emu.g^{-1})	M_r (emu.g^{-1})
BAl-0	4.20	88.00	53.50
BAl-2	3.13	45.00	27.00
BAl-4	2.85	43.00	26.50

The reflection loss of electromagnetic wave (for the case of a metal-backed single layer) can be calculated through the mathematical equation approach as follows:

$$R_L\,(-dB) = 20log\frac{|z_{in}-1|}{|z_{in}+1|} \quad \text{..... (2)}$$

with Z_{in} given by

$$Z_{in} = \sqrt{\frac{\mu_r}{\varepsilon_r}}\tanh\left[j\frac{2\pi}{c}\sqrt{\mu_r\varepsilon_r}fd\right] \quad \text{..... (3)}$$

where μ_r and ε_r are the complex magnetic permeability and electric permittivity of the medium, c is the velocity of light in free space, f is the frequency and d is the absorber thickness [1, 8].

The variation in reflection loss (RL) with frequency for all samples of 2.0 mm thickness in the frequency range of 9.0–13 GHz is shown in Figure 7. It can be seen that all compositions have reflection dip in the studied frequency range. The observed reflection loss RL is varying from -10.0 dB for Bal-0 to -36.0 dB for BAl-2 at 11.0 GHz frequency. Thus, these reflection losses dip shows that Al-substitution improves the absorption property of M-type ferrite.

The values of the RL peaks of the samples are listed in the Table 3. The RL for BAl-0 sample low for all the frequencies with a minimum value of RL −10 dB at 11.2 GHz. The RL is evidently improved to a minimum value of −35.00 dB at 11.00 GHz for BAl-2 with a bandwidth of 11.2 GHz, and increase to value of -32.0 for addition of Al doping x = 4.0 for BAl-4. The maximum RL value indicates that the absorption condition is satisfied where the value of complex electric permittivity (ε_r) and magnetic permeability (μ_r) in the BAl-2 are almost equal. The maximum absorption behavior of substituted M-type barium ferrites, BAl-2 and BAl-4 samples can be associated with the reduction of the magnetic coercivity and the particle size as compared to origin M-type barium ferrites BAl-0 sample.

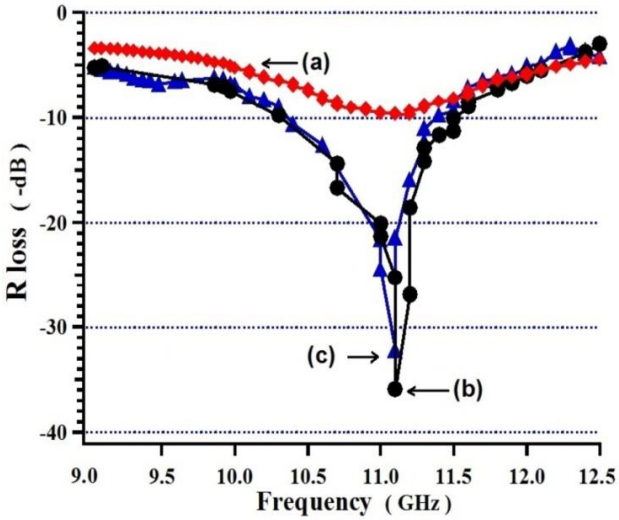

Figure 6 Reflection loss (-dB) versus frequencies (GHz) of M-type barium ferrite of (a). BAL-0, (b). BAl-2, and (c). BAl-4 samples

Table 3 Absorption properties of the samples

Samples/Al-doped (x)	BAl-0 x = 0.0	BAl-2 x = 2.0	BAl-4 x = 4.0
Frequency (GHz)	11.2	11.2	11.0
RL (-dB)	10.0	35.0	32.0

4.0 CONCLUSION

$BaFe_{12}O_{19}$ (BAl-0), $BaFe_{10}Al_2O_{19}$ (BAl-2) and $BaFe_8Al_4O_{19}$ (BAl-4) have been synthesized with solid state reaction technique using high energy milling (HEM) method. The XRD pattern reveals the formation of single M-type barium ferrite phase structure for all samples. Phase refinement was found to shrinkage in the lattice parameters "$a = b$" and volume cell (V_{cell}) with Al^{3+} substitution, while the lattice parameters "c" slight increase-decrease. The M-H curves recorded at room temperature exhibits a typical hysteresis loop indicating that the sample exhibits ferromagnetic nature. All the magnetic properties such as saturation magnetization (M_s), remanence magnetization (M_r) and coercivity (H_c) decreased in all samples with the increase of Al^{3+} content (x). The average particle size of the samples calculated using the Debye-Scherrer's formula was calculated in the range of 69 nm, 73 nm and 67 nm. The maximum absorption behavior of substituted M-type barium ferrites for $BaFe_{10}Al_20_{19}$ (BAl-2) sample at the frequencies of 11.0 GHZ exhibited the RL peak of -36dB.

Acknowledgement

This research was conducted by research and development of Smart magnetic Materials (DIPA, 2016-2017) in Center for Science and Technology of Advanced Materials – National Nuclear Energy Agency Indonesia.

References

[1] Z. W. Li, Z. H. Yang, and L. B. Kong. 2014. High-Frequency Properties and Electromagnetic Wave Attenuation for Hexaferrite Compsites. *Procedia Eng.* 75: 19-23.

[2] T. Ben Ghzaiel, Wadia Dhaoui, Alexandre Pasko, and Frederic Mazaleyrat. 2016. Effect of Non-magnetic and Magnetic Trivalent Ion Substitutions on BaM-ferrite Properties Synthesized by Hydrothermal Method. *J. Alloys Compd.* 671: 245-253.

[3] D. A. Vinnik, D. A. Zherebtsov, L. S. Mashkovtseva, S. Nemrava, M. Bischoff, E. N.S. Perov c, A. S. Semisalova, I. V. Krivtsov, L. I. Isaenko, G. G. Mikhailov, and R. Niewa. 2014. Growth, Structural and Magnetic Characterization of Al-Substituted Barium Hexaferrite Single Crystals. *J. Alloy. Compd.* 615: 1043-1046.

[4] Kanagesan, S, H. Mansor, and J. Sinnappan. 2014. Microwave Sintering of Zn-Nb Doped Barium Hexaferrite Synthesized via Sol-Gel Method. *Mater. Sci. Appl.* 5(March): 171-176.

[5] S. Kanagesan, M. Hashim, T. Kalaivani, I. Ismail, and N. Rodziah. 2014. Microwave Sintering of Ni-Cr Doped Strontium Hexaferrite Synthesized via SOL-GEL Method. *World Appl. Sci. J.* 32(5): 916-920.

[6] S. Malhotra, M. Chitkara, and I. S. Sandhu. 2015. Microwave Absorption Study of Nano Synthesized Strontium Ferrite Particles in X Band. *Int. J. Signal Process.* 8(10): 115-120.

[7] S. Das, G. C. Nayak, P. C. Routray, A. K. Roy, and B. H. 2014. Microwave Absorption Properties of Double-Layer RADAR Absorbing Materials Based on Doped Barium Hexaferrite/TiO2/Conducting Carbon Black. *J. Eng.* 2014,

[8] S. R. M. M. Ghimire, S. Yoon, L. Wang, D. Neupane, J. Alam. 2018. Influence of La Content on Magnetic Properties of Cu Doped M-type Strontium Hexaferrite: Structural, Magnetic, and Mossbauer Spectroscopy Study. *J. Magn. Magn. Mater.* https//doi.org/10.1016/j.jmmm.2018.01.062.

[9] C. P. Santhoshkumar Mahadevan, S. B. Narang, and P. Sharma, 2017. Structural, Dielectric and Magnetic Properties of BaFe12-xAlxO19 Hexaferrite Thick Films. *J. Magn. Magn. Mater.* http//dx.doi.org/10.1016/j.jmmm.2017.05.087.

[10] A. V. Trukhanov, S. V. Trukhanov, L. V. Panina, V. G. Kostishyn, I. S. Kazakevich, V. A. Turchenko, M. M. Salem, and A. M. Balagurov. 2016. Evolution of Structure and Magnetic Properties for BaFe11.9Al0.1O19 Hexaferrite in a Wide Tempreture Range. *J. Magn. Magn. Mater.* http//dx.doi.org/10.1016/j.jmmm.2016.10.140.

[11] Y. Yang, F. Wang, X. Liu, J. Shao, and D. Huang. 2016. Magnetic and Microstructural Properties of Al Substituted M-type Ca-Sr Hexaferrites. *J. Magn. Magn. Mater.* http//dx.doi.org/10.1016/j.jmmm.2016.08.034.

[12] A. Hoodaa, S. Sanghi, A. Agarwal, and R. Dahiya. 2016. Crystal Structure Refinement, Dielectric and Magnetic Properties of Ca/ Pb Substituted SrFe12O19 Hexaferrites. *J. Magn. Magn. Mater.* 412: 69-82.

[13] Winatapura D. S, Ujiyanti T. L, and Wisnu Ari Adi. 2017. The Structure, Magnetic and Absorption Properties of Zn-Ti Substituted Barium-Strontuim Hexaferrite Prepared by Mechanochemical. *IOP Conf. Series: Materials Science and Engineering 202 012090.* 2017. 1-10. doi: 10.1088/1757-899X/202/1/012090.

[14] A. V Trukhanov, L. V Panina, S. V Trukhanov, V. O. Turchenko, I. S. Kazakevich, and M. M. Salem. 2015. Features of Crystal Structure and Magnetic Properties of M-type Ba-hexaferrites with Diamagnetic Substitution. *Int. J. Mater. Chem. Phys.* 1(3): 286-294.

[15] R. C. Alange, P. P. Khirade, S. D. Birajdar, A. V. Humbe, and K. M. J. B. 2016. Structural, Magnetic and Dielectrical Properties of Al-Cr- Co Substituted M-type Barium Hexaferrite Nanoparticles. *J. Mol. Struct.* 1106: 460-467.